

# EgoVITA: Learning to Plan and Verify for Egocentric Video Reasoning

# Yogesh Kulkarni Pooyan Fazli Arizona State University

{ykulka10, pooyan}@asu.edu

https://people-robots.github.io/EgoVITA/

# **Abstract**

Reasoning about intentions and actions from a first-person (egocentric) perspective remains a fundamental challenge for multimodal large language models (MLLMs). Unlike third-person (exocentric) videos that capture scenes from an outside observer, egocentric videos reflect the actor's continuously changing viewpoint, introducing partial observability, limited field of view, and self-referenced motion. We introduce EgoVITA, a reinforcement learning framework that enables MLLMs to reason through structured planning and verification. Built on Group Relative Policy Optimization (GRPO), EgoVITA alternates between two stages: (1) an egocentric planning phase, where the model reasons from a first-person viewpoint to predict a step-by-step plan of future actions, and (2) an exocentric verification phase, where it switches to a third-person perspective to check the visual and logical consistency of that plan. Through GRPO, the model learns to make plans that are causally predictive of upcoming visual observations, leading to more coherent and visually grounded reasoning. EgoVITA achieves significant gains on egocentric reasoning tasks, outperforming the baseline Qwen2.5-VL-7B by +7.7 on EgoBlind and +4.4on EgoOrient, while maintaining strong generalization on exocentric video tasks.

# 1. Introduction

Egocentric, or first-person, videos play a central role in applications such as life-logging, personal memory assistants [40], assistive technology [14, 37], robot learning [47], sports analysis [3], and immersive AR/VR experiences [44]. Interpreting these videos is challenging due to constant camera motion, limited field of view, and frequent occlusions. Effective understanding requires procedural reasoning, the ability to predict action outcomes, infer goals, and reason about object interactions over time. However, current multimodal large language models (MLLMs) show significant weak-



**Query:** As a blind guide dog user, how would you safely enter the SUV's second row without verbal help using only your cane and Yuki's harness?

**Qwen2.5-VL:** Walk straight in and let the dog jump first since the car is small, someone will move you if you block the door.

**EgoVITA:** Grip the door frame to stabilize your entry, sweep the cane to confirm the step-in point and aisle width, then guide Yuki left into the footwell where the spacious legroom ensures she stays clear of the pathway without obstructing your seat access.

Figure 1. **EgoVITA enables safer, structured egocentric reasoning.** For a first-person query, it produces a grounded, stepwise plan anticipating actions and spatial constraints, whereas Qwen2.5-VL gives generic, unsafe, visually ungrounded responses.

nesses in first-person video understanding. They frequently generate plausible but incorrect descriptions [30], show weak spatiotemporal reasoning [20, 21, 28], poor memory of object states [42], and limited understanding of user goals and intentions [19, 26, 32]. Their accuracy also remains low on scene-text reading [46], object orientation [7, 12], and crossview alignment [9], lagging far behind human performance even on large-scale, challenging benchmarks such as HD-EPIC [27]. These shortcomings reveal a key gap: current MLLMs lack mechanisms to model how actions, objects, and observations evolve from a first-person perspective. While supervised fine-tuning (SFT) on egocentric datasets can improve performance, it often reduces accuracy on standard exocentric benchmarks. This trade-off highlights the broader challenge of viewpoint generalization and the need for models that reason effectively from an egocentric perspective without losing exocentric competence.

We argue that robust egocentric reasoning requires moving beyond SFT, which merely imitates fixed action sequences. Effective reasoning is outcome-driven: the model must generate action sequences whose combined effect achieves the desired goal, making success dependent on the

coherence of the entire sequence. Methods like Direct Preference Optimization (DPO) [15, 17, 29] improve on SFT by ranking candidate sequences. However, DPO is offline and limited to pre-collected data with feedback reflecting relative preferences rather than the actual trajectory success. This restricts the model's ability to explore novel sequences or adapt to unseen scenarios. In contrast, reinforcement learning (RL) provides true outcome-driven optimization, where feedback is based on the success of actions generated by the agent. In particular, Group Relative Policy Optimization (GRPO) [8] enhances standard RL by evaluating trajectories within a group using relative rewards, providing denser, more stable learning signals. This enables the model to explore new reasoning paths, maintain temporal and causal consistency, and generalize to unseen situations [16].

We introduce **EgoVITA** (**Ego**centric **V**ideo **I**ntelligence and **T**hinking **A**gent), a reinforcement learning framework for structured multimodal reasoning on egocentric videos based on GRPO. The model first generates an *egocentric plan*, outlining intended actions from a first-person perspective, and then performs an *exocentric verification*, evaluating the plan from a third-person viewpoint to ensure consistency with visual evidence and task goals. This two-stage design encourages the model to learn view-invariant representations without requiring synchronized egocentric and exocentric video pairs [13]. Notably, we introduce dense, task-aware rewards, which stabilize learning, improve first-person video reasoning, and support strong cross-view generalization. In summary, our contributions are as follows:

- 1. We propose EgoVITA, an RL framework that decomposes egocentric reasoning into an egocentric planning stage and an exocentric verification stage.
- 2. We introduce two novel dense rewards to guide this process: one encourages the *planning* stage to accurately predict future visual frames, and the other refines the *verification* stage by promoting logical coherence.
- 3. We show that EgoVITA functions as a unified, view-invariant model, achieving significant gains on five egocentric benchmarks (e.g., +7.7 on EgoBlind) and four exocentric benchmarks (e.g., +2.4 on VideoMME).

# 2. Related Work

Egocentric Video Understanding. Egocentric video reasoning is uniquely challenging due to rapid camera motion, frequent object occlusions [20, 27], and the need to infer the intentions of an unobserved, active person [25, 32]. As a result, recent MLLM research has focused mainly on creating *benchmarks* that highlight specific cognitive failures rather than developing new *methods*. These failures include deficits in long-term memory and procedural reasoning [33, 40, 41], fundamental temporal understanding [28], spatial orientation [7, 12], and intention or Theory of Mind grounding [19, 26, 32]. Models also struggle with fine-

grained perception of dynamic object states [42] or scenetext [46], and often show hallucinations [30] or provide unsafe answers in assistive contexts [14, 37]. The few methods proposed, such as EgoThinker [25] and EgoVLM [34], employ reinforcement learning. However, their reliance on simple, sparse rewards for output format and correctness limits long-term procedural reasoning and often causes catastrophic forgetting of general exocentric knowledge. To address this, we introduce a novel framework that leverages dense, predictive rewards to teach complex egocentric procedures while preserving exocentric generalization, tackling a key challenge in ego-exo knowledge transfer [10, 23, 43].

Ego-Exo Video Understanding. Applying MLLMs trained on large corpora of exocentric images and videos to egocentric video faces a fundamental ego-exo gap [9]. This domain shift introduces several challenges, including viewpoint disparity that disrupts feature alignment [23], difficulty in matching objects across views [24], and complications in relative spatial reasoning [7]. Prior work attempts to bridge this gap by learning view-invariant representations [23], using audio as a "sound bridge" [10], or employing SFT pipelines for direct knowledge transfer [39, 43]. While these approaches improve cross-view alignment, they struggle to teach dynamic procedural reasoning and often suffer from catastrophic forgetting of exocentric knowledge during finetuning. EgoVITA overcomes these limitations by explicitly separating reasoning into an egocentric planning phase and an exocentric verification phase. This design enables the model to learn robust first-person understanding while using verification to preserve third-person generalization. Unlike prior work [13] that relies on synchronized ego-exo video pairs, EgoVITA achieves scalable cross-view consistency without requiring paired data.

# 3. EgoVITA



We introduce EgoVITA, a framework that enables MLLMs to reason effectively about egocentric video. EgoVITA is trained in two stages. In *Stage I*, SFT establishes a stable base policy capable of generating structured outputs. In *Stage II*, this policy is refined using GRPO by exploring diverse reasoning trajectories and their relative performance. The framework separates reasoning into two complementary components. First, **egocentric planning** operates from a first-person viewpoint to generate an explicit plan of anticipated actions. Second, **exocentric verification** uses a third-person perspective to evaluate the plan for visual and logical consistency. Trained with novel dense rewards that capture future visual states and task outcomes, EgoVITA achieves stable learning and robust egocentric understanding. The overall framework is illustrated in Figure 2.

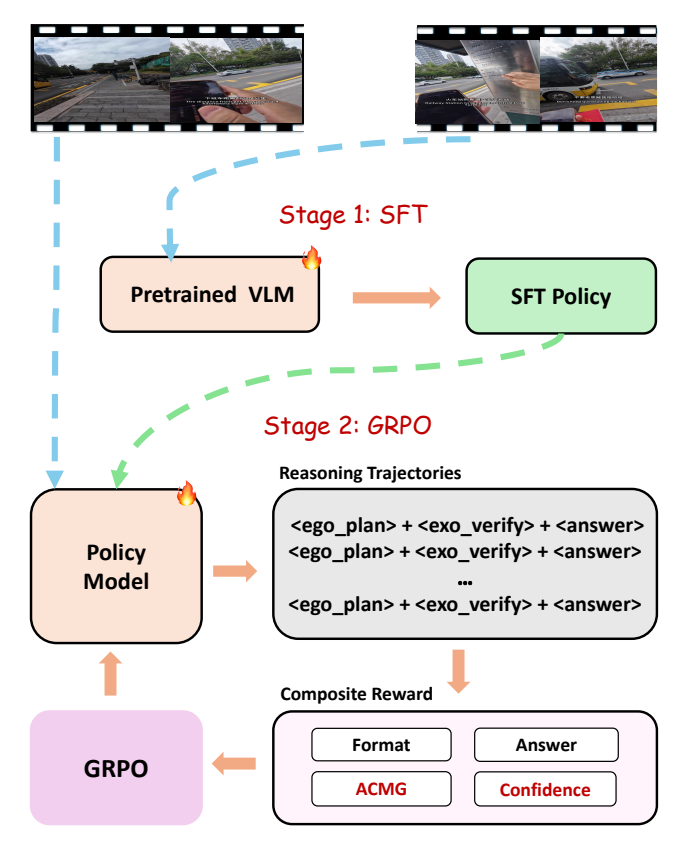


Figure 2. **EgoVITA** training pipeline. In Stage I SFT, the policy model is initialized to learn the structured <ego\_plan>, <exo\_verify>, and <answer> format. In Stage II GRPO, it generates reasoning trajectories for a given video and query, scores them with a composite reward, and refines the model accordingly.

### 3.1. Problem Formulation

We formulate egocentric video reasoning as a sequential decision-making problem. The MLLM acts as a policy  $\pi_{\theta}$ , parameterized by weights  $\theta$ . Given an input video V and a text prompt X, the policy autoregressively generates a reasoning trajectory  $Y = \langle y_1, \ldots, y_T \rangle$ , where each token  $y_t$  represents a reasoning step conditioned on the video, prompt, and prior steps  $y_t \sim \pi_{\theta}(y_t \mid V, X, y_{< t})$ . Each trajectory Y is a sequence consisting of an egocentric plan (egoplan>), an exocentric verification (exoverify>), and an answer (exoverify>) block. The quality of a generated sequence Y is evaluated by a composite reward function R that combines syntactic, semantic, and visual signals to assess overall reasoning quality. The objective is to learn a policy that maximizes the expected reward:

$$\theta^* = \arg\max_{\theta} \mathbb{E}_{Y \sim \pi_{\theta}(Y|V,X)}[R(Y)]. \tag{1}$$

### 3.2. Stage I: SFT

SFT establishes a stable initial policy  $\pi_{SFT}$  by training the MLLM to perform two complementary reasoning skills: *ego*-

centric planning and exocentric verification. This stage helps the model learn how to plan and verify effectively while becoming familiar with the structured output format (i.e., generating text within <ego\_plan>, <exo\_verify>, and <answer> tags). By grounding the model in these reasoning patterns, SFT initializes the policy in a well-conditioned region of the parameter space, which improves the stability and effectiveness of GRPO optimization for Stage II.

Egocentric Planning. To train the model to generate feasible plans and temporally grounded action sequences from a first-person viewpoint, we use the EgoProceL dataset [2], which provides time-aligned action annotations for egocentric videos. Each sample includes a query (e.g., "How do I prepare the vegetables for cooking?") paired with a ground-truth plan formatted as an instruction-following sequence (e.g., <ego\_plan> 1. Pick up the knife. 2. Place it on the board. </ego\_plan>). We use Qwen2.5-VL-72B model [1] to generate the egocentric plans leveraging the ground truth data (Prompt provided in Supp.).

**Exocentric Verification.** To train the model to verify plans against visual evidence, we construct a dataset using HD-EPIC [27] and the Qwen2.5-VL-72B model [1]. For each egocentric video clip in HD-EPIC, Qwen2.5-VL-72B generates a chain-of-thought rationale from a third-person perspective, leveraging human-annotated ground truth to ensure factual grounding (Prompt provided in Supp.). For example: <exo\_verify> The plan is valid because the knife is visible on the counter. </exo\_verify>. This process teaches the model to assess the logical and visual consistency of its plans, complementing planning with external verification.

**Joint SFT Objective.** We merge both datasets into a unified corpus, D, and train the policy using standard cross-entropy loss:

$$\mathcal{L}_{SFT}(\theta) = -\mathbb{E}_{(V,X,Y^*) \sim D} \left[ \log \pi_{\theta}(Y^* \mid V, X) \right], \quad (2)$$

where  $(V, X, Y^*)$  denotes a video, prompt, and ground-truth reasoning sequence. Training on the combined corpus lets the model learn planning and verification simultaneously.

# 3.3. Stage II: GRPO

After SFT, we refine the policy  $\pi_{\theta}$  using GRPO, which improves reasoning by exploring and evaluating multiple candidate plans. In egocentric video understanding, there is rarely a single correct reasoning path, since several plausible interpretations can arise depending on context and camera motion. GRPO addresses this by sampling a group of trajectories per input and updating the policy based on their relative rewards, promoting diverse exploration while keeping learning stable.

### 3.3.1. GRPO Rollouts, Rewards, and Policy Updates

For each video-prompt pair (V, X), the policy  $\pi_{\theta}$  generates a group of k = 8 rollouts  $\{Y_1, \dots, Y_k\}$ , where each

sequence includes a full <ego\_plan>, <exo\_verify>, and <answer> block. Each  $Y_i$  is scored using a *composite reward* R that combines syntactic, semantic, and visual signals to assess overall reasoning quality.

**Composite Reward** (R). The reward is a weighted sum of four components:

$$R = w_f R_{\text{format}} + w_a R_{\text{answer}} + w_q R_{\text{ACMG}} + w_c R_{\text{confidence}}, \quad (3)$$

where:

- 1. Format Reward ( $R_{\text{format}}$ ) is a sparse binary reward that checks for correct tag usage and output structure,
- 2. Answer Reward ( $R_{
  m answer}$ ) is a sparse reward measuring factual alignment between the generated and ground-truth answer choices,
- 3. **ACMG Reward** ( $R_{\rm ACMG}$ ) is a dense reward promoting temporal and visual grounding of the predicted plan in future frames (Sec. 3.3.2), and
- 4. Confidence Reward ( $R_{\text{confidence}}$ ) is a dense reward encouraging coherent and consistent reasoning (Sec. 3.3.3).

Sparse rewards ( $R_{format}$ ,  $R_{answer}$ ) provide a single pass/fail score for the entire sequence, while our novel dense rewards ( $R_{ACMG}$ ,  $R_{confidence}$ ) provide continuous, stepwise feedback essential for learning complex planning.

**GRPO Objective.** Group-level rewards  $\{R(Y_i)\}_{i=1}^k$  are normalized to compute relative advantages:

$$\hat{A}(Y_i) = \frac{R(Y_i) - \mu_R}{\sigma_R + \epsilon},\tag{4}$$

where  $\mu_R$  and  $\sigma_R$  are the mean and standard deviation of the group rewards. The policy is then updated by minimizing the GRPO objective:

$$\mathcal{L}_{GRPO}(\theta) = \mathbb{E}_{Y \sim \pi_{\theta}} \left[ -\hat{A}(Y) \log \pi_{\theta}(Y \mid V, X) \right]$$
$$-\beta_{KL} D_{KL} \left( \pi_{\theta}(Y \mid V, X) \mid\mid \pi_{SFT}(Y \mid V, X) \right), \quad (5)$$

where  $\beta_{\rm KL}$  limits deviation from the stable SFT policy.

### 3.3.2. Anticipatory Cross-Modal Grounding (ACMG)

To ensure each generated <ego\_plan> is temporally predictive and visually grounded, we introduce the *Anticipatory Cross-Modal Grounding (ACMG)* reward. This self-supervised signal measures how well the generated plan anticipates future visual states (Figure 3).

**Mechanism.** Each <ego\_plan> is divided into semantic clauses  $c_i$  (e.g., "Pick up the knife"). For each clause, we extract its final hidden state  $h_i$  from the LLM and project it into the visual embedding space via a small trainable MLP (Anticipation Head) to predict the visual embedding of the next moment  $\hat{v}_i = \text{MLP}(h_i^{\text{text}})$ . The Anticipation Head

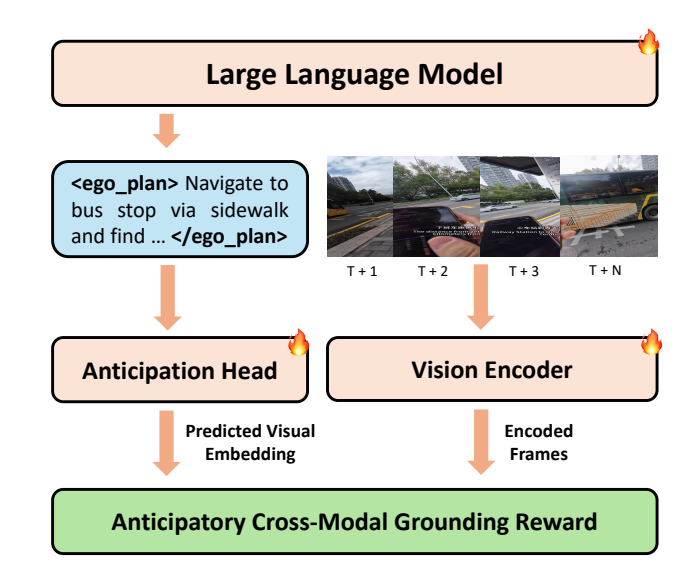


Figure 3. Anticipatory Cross-Modal Grounding (ACMG). The generated plan is projected into visual space via a trainable MLP (Anticipation Head) and compared to N future frames, encoded by the vision encoder, using cosine similarity. ACMG is the maximum similarity, encouraging plans that predict actual future observations. All components are trained jointly under GRPO.

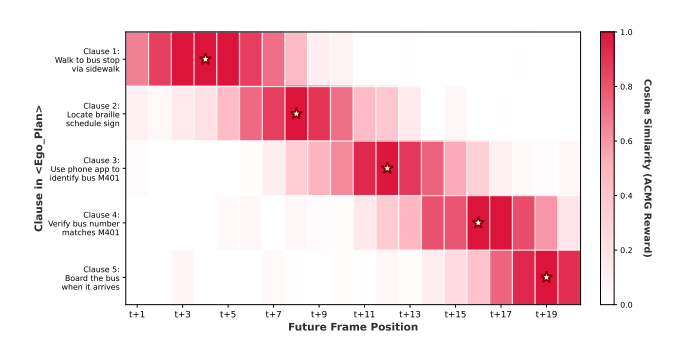


Figure 4. **Temporal Grounding via ACMG.** Heatmap shows cosine similarity between each clause's predicted visual embedding and N future frames. White stars indicate maximum similarity (best temporal match). ACMG rewards clauses that accurately predict future visual states, earlier clauses ground to near-future frames (e.g., Clause 1 peaks at t+4), while later clauses align with distant frames (Clause 5 peaks at t+19), demonstrating the model learns temporally structured anticipation.

operates on language embeddings already aligned with visual concepts through the MLLM's pretrained cross-attention layers, enabling direct mapping between textual descriptions (e.g., "knife") and their corresponding visual representations. We then encode the next N=16 frames following the current timestamp t with the trainable vision encoder to obtain embeddings  $\{v_{t+1},\ldots,v_{t+N}\}$ . The ACMG reward for each clause  $c_i$  measures how closely its predicted feature matches any of these future frames using cosine similarity:

$$R_{\text{ACMG}}(c_i) = \max_{n \in \{1, \dots, N\}} \frac{\hat{v}_i \cdot v_{t+n}}{\|\hat{v}_i\| \|v_{t+n}\|}.$$
 (6)

The max operation selects the best-aligned frame (e.g., when the knife enters view), making the reward robust to temporal shifts and irrelevant frames. As shown in Figure 4, earlier clauses align with near-future frames, while later ones match more distant events. For a trajectory with K clauses  $C = \{c_1, \ldots, c_K\}$  extracted from <ego\_plan>, the ACMG reward is the mean across all clauses:

$$R_{\text{ACMG}} = \frac{1}{K} \sum_{i=1}^{K} \max_{n=1}^{N} \text{sim}(\hat{v}_i, v_{t+n}).$$
 (7)

# 3.3.3. Confidence Reward

To improve the logical coherence of <exo\_verify>, we introduce a *confidence reward* computed from the policy model's log-probabilities.

**Teacher-guided phase.** During the first 200 RL steps, for each sample, each of the k=8 rollout verifications is compared to a teacher-generated reference verification. This reward guides the model to match the teacher's reasoning quality:

$$R_{\text{confidence}} = \beta \cdot \left[ \log \pi_{\theta}(y^{\mathsf{T}} \mid X) - \log \pi_{\theta}(y^{\mathsf{P}} \mid X) \right], (8)$$

where  $y^{\rm T}$  and  $y^{\rm P}$  denote teacher and policy outputs, respectively. We use Qwen2.5-VL-72B [1] as the teacher. This phase helps the model learn stable and coherent verification before self-improvement begins.

**Self-ranking phase.** After the warm-up, each of the k=8 rollout verification is scored using the composite reward (Eq. 3), and the highest-  $(y^{\rm chosen})$  and lowest-scoring  $(y^{\rm rejected})$  outputs are compared:

$$R_{\text{confidence}} = \begin{cases} \beta \cdot (\log \pi_{\theta}(y_{\text{chosen}} \mid X) \\ -\log \pi_{\theta}(y_{\text{rejected}} \mid X)), & \text{if scores differ;} \\ 1, & \text{otherwise.} \end{cases}$$

This adaptive setup first grounds the model in teacher examples, then encourages self-improvement by favoring outputs with higher confidence. The teacher is used only during the early warm-up phase for verification, not for planning.

# 3.4. Exocentric Regularization

Training solely on egocentric data can lead to *catastrophic* forgetting, degrading the model's general exocentric understanding. To mitigate this, we periodically interleave GRPO updates with a lightweight exocentric regularization step. Specifically, after every 200 RL iterations, the model is evaluated on a held-out exocentric VideoQA dataset

(MSRVTT [38]) using a cross-entropy loss  $\mathcal{L}_{\rm exo}$ . This loss is combined with the GRPO objective:

$$\mathcal{L}_{\text{total}} = \mathcal{L}_{\text{GRPO}} + \lambda_{\text{exo}} \mathcal{L}_{\text{exo}}.$$
 (10)

This multi-task constraint preserves general visual reasoning while allowing specialization to egocentric tasks.

# 4. Experiments and Evaluation

**Implementation Details.** We implement EgoVITA using the open-source MS-SWIFT [45] library. In Stage I (SFT). we train on two datasets: EgoProceL [2] (5k samples)for planning and HD-EPIC [27] (7k samples) for verification. Chain-of-thought reasoning traces for Stage I (planning and verification) are generated by Qwen2.5-VL-72B [1] using ground-truth annotations. The SFT model is trained for one epoch with a learning rate of 5e-6. In Stage II (GRPO), we use HD-EPIC and EgoIT (40k samples) [40] as rollout sources, setting the policy temperature  $\beta = 0.1$  and the exocentric regularization coefficient  $\lambda_{\rm exo} = 0.05$ . We apply EgoVITA to three state-of-the-art MLLMs: Qwen2.5-VL-7B [1], InternVL3.5-8B [35], and Qwen3-VL-8B. All models are trained on 8 NVIDIA L40S GPUs using DoRA [22] adapters (r = 8,  $\alpha = 16$ ) on the vision encoder, projector, and the LLM. The reward weights are set to  $\{w_f, w_a, w_a, w_c\} = \{0.1, 0.3, 0.3, 0.3\}.$ 

Benchmarks. We evaluate EgoVITA on several egocentric video understanding benchmarks, including EgoBlind [37] (first-person visual assistance for blind users), EgoPlan [4] (egocentric task planning), EgoThink [5] (first-person perspective thinking capability), and EoC-Bench [42] (object-centric embodied cognition across past, present, and future). To assess cross-view generalization, we also evaluate on standard exocentric video understanding benchmarks: MVBench [18] (temporal perception-to-cognition QA), Video-MME [6] (comprehensive video understanding), LVBench [36] (long-video understanding and reasoning), and TOMATO [31] (visual temporal reasoning).

### 4.1. Results

We compare EgoVITA against four baselines: (1) the original foundation models, (2) the same models after SFT, (3) the SFT models further trained with GRPO using only final-answer and format rewards, and (4) state-of-the-art MLLMs for egocentric video understanding.

**EgoVITA improves all foundation models.** As shown in Table 1, EgoVITA consistently enhances egocentric video understanding across all tested foundation models. For instance, on InternVL-3.5, it achieves substantial gains of +3.6 on EgoBlind and +3.8 on EgoOrient, demonstrating enhanced egocentric reasoning. For Qwen2.5-VL, it delivers significant improvements, with gains of +7.7 points on

Table 1. Evaluation of EgoVITA on egocentric and exocentric benchmarks across different foundation models. Best scores are in bold, and improvements from EgoVITA are highlighted in green with 95% confidence interval (CI) margins ( $\pm$ ) computed via bootstrap resampling (10,000 iterations, percentile method). Improvements are statistically significant at  $\alpha = 0.05$  when CIs exclude zero. Baseline GRPO uses only format and answer rewards. <sup>‡</sup> Improvement not statistically significant (p > 0.05; 95% CI includes zero).

		Egocer	ntric Video Unders	tanding			Exocentric Vide	eo Understanding	
Model	EgoBlind	EgoPlan	EgoThink	EOC-Bench	EgoOrient	MVBench	Video-MME	LVBench	Tomato
				InternVL-3.5	Family				
InternVL-3.5	47.8	34.0	58.5	37.1	36.3	71.4	65.6	44.4	31.4
SFT	49.2	34.8	59.3	38.1	37.8	68.2	62.1	41.2	29.8
GRPO (Format + Answer)	49.8	35.1	59.6	38.6	38.4	68.9	63.2	41.8	30.1
EgoVITA	51.4 (+3.6±0.5)	35.9 (+1.9 $\pm$ 0.5)	60.8 (+2.3±0.5)	39.7 (+2.6±0.6)	40.1 (+3.8±0.7)	73.8 (+2.4±0.6)	68.3 (+2.7±0.6)	47.1 (+2.7±0.7)	33.2 (+1.8±0.6
				Qwen2.5-VL	Family				
Qwen2.5-VL	29.7	30.2	48.2	41.6	47.6	65.2	62.2	42.8	29.3
SFT	34.8	31.3	49.1	41.8	48.1	63.2	60.1	40.2	29.0
GRPO (Format + Answer)	35.6	31.4	49.0	42.2	48.6	66.4	62.9	40.9	29.8
EgoVITA	37.4 (+7.7±0.9)	32.9 (+2.7±0.6)	51.9 (+3.7±0.7)	44.1 (+2.5±0.6)	52.0 (+4.4±0.8)	66.8 (+1.6±0.5)	64.6 (+2.4±0.6)	43.6 (+0.8 ± 0.5)	30.2 (+0.9±0.5
				Qwen3-VL F	Family				
Qwen3-VL	48.4	33.7	62.7	46.8	60.8	68.4	71.4	56.1	34.0
SFT	50.1	34.2	63.1	47.5	61.8	68.2	71.2	56.3	34.2
GRPO (Format + Answer)	50.8	34.5	63.4	47.9	62.3	68.1	71.1	56.4	34.3
EgoVITA	51.9 (+3.5±0.7)	35.0 (+1.3 ± 0.5)	63.9 (+1.2±0.5)	48.6 (+1.8 ± 0.6)	63.1 (+2.3 ± 0.6)	69.2 (+0.8 ± 0.5)	72.2 (+0.8 ± 0.5)	56.5 (+0.4±0.4)‡	34.5 (+0.5±0.4

Table 2. **EgoVITA vs. state-of-the-art egocentric reasoning MLLMs**. Numbers reported from original papers.

Model	EgoPlan	EgoSchema	MVBench	Video-MME
EgoThinker [25]	33.1	67.6	70.0	62.9
EgoVLM [34]	33.8	74.0	66.5	_
EgoVITA	35.0	75.8	69.2	72.2

EgoBlind, +3.7 on EgoThink, and +4.4 on EgoOrient, indicating that our framework effectively strengthens temporal grounding and procedural reasoning. The trend persists with the stronger Qwen3-VL, which achieves notable gains of +3.5 on EgoBlind and +2.3 on EgoOrient, showing that the benefits generalize to more capable base models. These results confirm that EgoVITA achieves a model-agnostic alignment strategy that generalizes across diverse foundation models with improvements that are statistically significant (p < 0.05) across all models.

Comparison with SFT. As shown in Table 1, SFT alone yields only minor gains on egocentric while degrading exocentric understanding. For instance, on Qwen2.5-VL, SFT reduces performance by −2.0 on MVBench and −2.1 on Video-MME, both exocentric video understanding benchmarks, compared to the base model. This drop occurs because SFT overfits to egocentric data distributions and lacks feedback mechanisms to preserve general reasoning skills. In contrast, EgoVITA incorporates continuous reward signals from both visual grounding and confidence alignment, enabling the model to improve egocentric reasoning without forgetting exocentric perception. Notably, EgoVITA improves InternVL-3.5 performance to 51.4 on EgoBlind

(vs. 49.2 with SFT) and even yields a +2.7 point gain on VideoMME and LVBench showing that exocentric regularization helps preserve exocentric visual understanding.

Comparison with GRPO (Format + Answer). To isolate the effect of our reward design, we compare EgoVITA with a GRPO baseline trained using only format and answer rewards. This baseline provides only marginal gains over SFT, as it optimizes for output format and final correctness rather than reasoning quality. In contrast, adding our dense multimodal rewards, including ACMG for temporally predictive egocentric planning and confidence for exocentric verification, leads to substantial improvements. For instance, on InternVL-3.5, EgoVITA outperforms GRPO by +1.6 on EgoBlind and +1.7 on EgoOrient. Similarly, on Qwen2.5-VL, it achieves gains of +1.8 on EgoBlind and +3.4 on EgoOrient. These results demonstrate that grounding reasoning in future visual context and reinforcing self-verification are both essential for robust egocentric understanding.

Comparison with Egocentric Reasoning Models. Table 2 compares EgoVITA with recent egocentric reasoning models. Both EgoThinker [25] and EgoVLM [34] rely on sparse, rule-based rewards for RL training, whereas EgoVITA introduces dense ACMG and confidence rewards to guide planning and verification. Despite requiring far fewer training samples (47k) than EgoThinker (5M), EgoVITA achieves higher accuracy on EgoSchema (75.8 vs. 67.6) and EgoPlan (35.0 vs. 33.1). It also outperforms EgoVLM on both benchmarks (75.8 vs. 74.0 on EgoSchema and 35.0 vs. 33.8 on EgoPlan). These results show that our model learns to correct *how* it reasons, not just *what* it answers.

Table 3. ACMG and Confidence Rewards on Qwen2.5-VL. Removing either reward reduces grounded reasoning performance.

Variant	EgoPlan	EOC-Bench	Video-MME	Tomato
GRPO (Format + Answer)	31.4	42.2	62.9	29.8
+ ACMG only	32.0	43.1	63.4	29.9
+ Confidence only	32.3	43.5	63.8	30.0
EgoVITA (Full)	32.9 (+1.5)	44.1 (+1.9)	64.6 (+1.7)	30.2 (+0.4)

Table 4. **Disentangled reasoning.** Removing <ego\_plan> harms egocentric reasoning, while removing <exo\_verify> reduces exocentric performance, showing their complementary roles.

Variant	EgoPlan	EOC-Bench	Video-MME	Tomato
GRPO (Format + Answer)	31.4	42.2	62.9	29.8
w/o <ego_plan></ego_plan>	29.6	40.1	63.0	29.7
w/o <exo_verify></exo_verify>	31.5	42.5	61.2	28.3
EgoVITA (Full)	32.9 (+1.5)	44.1 (+1.9)	64.6 (+1.7)	30.2 (+0.4)

### 4.2. Ablation Studies

RQ1: Are ACMG and confidence rewards complementary? Table 3 shows that adding ACMG alone to GRPO (Format + Answer) improves performance by +0.6 on Ego-Plan and +0.9 on EOC-Bench, while confidence reward alone yields gains of +0.9 and +1.3, respectively. When combined, EgoVITA achieves +1.5 on EgoPlan and +1.9on EOC-Bench, exceeding the improvements of each individually. This indicates that ACMG and confidence rewards are complementary. ACMG grounds egocentric plans in anticipated visual outcomes by rewarding clauses that accurately predict future frames, while the confidence reward strengthens logical consistency and exocentric verification through log-probability alignment. These multimodal rewards improve egocentric reasoning and generalize effectively to exocentric understanding, yielding a +1.7 gain on Video-MME, demonstrating enhanced overall reasoning robustness.

RQ2: Is disentangled reasoning into <ego\_plan> and <exo\_verify> necessary? Yes. Table 4 shows that disentangled reasoning is essential for balanced performance. Removing <ego\_plan> degrades egocentric performance compared to GRPO (Format + Award) (-1.8 on EgoPlan, -2.1 on EOC-Bench) while exocentric performance remains nearly unchanged, indicating that first-person procedural reasoning benefits from an explicit planning structure. Conversely, removing <exo\_verify> preserves egocentric performance (+0.1 on EgoPlan) but reduces exocentric understanding (-1.7 on Video-MME, -1.5 on Tomato), confirming that third-person verification is critical for general visual reasoning. These results validate our architectural choice: <ego\_plan> enables temporally grounded reasoning from the first-person perspective, while <exo\_verify> provides an objective verification that generalizes to thirdperson tasks. The full EgoVITA framework combines both,

achieving improvements across all benchmarks (+1.5-1.9 on egocentric, +0.4-1.7 on exocentric). In the ablations, we maintain the same output format but remove only the specified component: without <ego\_plan>, the model generates <exo\_verify> only for the <answer>, whereas without <exo\_verify>, the model generates both <ego\_plan> and <answer>.

RO3: Does EgoVITA learn semantically structured visual-linguistic embeddings? To analyze the embedding space, we use GPT-40 [11] to categorize <ego\_plan> clauses from 75 EgoPlan [4] videos into five high-level procedural steps: Move  $\rightarrow$  Locate  $\rightarrow$  Action  $\rightarrow$  Verify  $\rightarrow$  Complete. This 5-step sequence is not rigid but reflects a common semantic structure in procedural tasks. Figure 5 shows that ACMG induces a clear semantic structure in the embeddings. First, it achieves between-cluster separation, with each procedural step forming a distinct cluster. Second, it achieves within-cluster alignment, where text clauses, predicted visual embeddings, and actual frames align closely. The proximity of predicted visual embeddings (red diamonds)  $\Diamond$  to actual frames (green stars) \* confirms that the Anticipation Head accurately maps textual plans to corresponding future visual states. A few outliers reflect minor timing prediction errors, but overall, the results show that EgoVITA learns meaningful, grounded task semantics. This structure is reflected in the qualitative examples (Figure 6). For example, in the blind crossing video, the <ego\_plan> maps sequentially to the five semantic categories: Move (approach intersection), Locate (identify curb edge), Action (sweep cane), Verify (confirm crosswalk), Complete (cross with steady pace).

# **RQ4:** Why does grounding in future frames (ACMG) improve procedural reasoning? ACMG trains the model

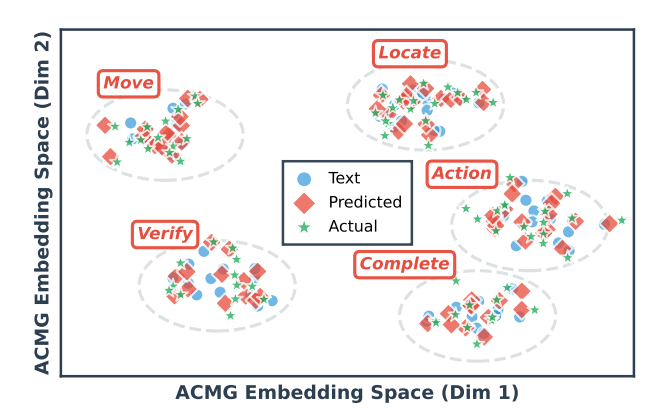


Figure 5. **ACMG Embedding Space Structure.** t-SNE projection of text clauses (blue circles), MLP-predicted embeddings (red diamonds), and their corresponding matched frames (green stars) from 75 egocentric video clauses. Distinct clusters emerge by action type, with strong alignment between predicted and actual embeddings, demonstrating effective cross-modal grounding.



**Query:** As a blind person, how can I safely cross this intersection without assistance?



**Query:** What systematic approach is being used for grapevine pruning in this video?

<ego\_plan> 1. Approach intersection while extending white cane to detect obstacles. 2. Identify curb edge through feedback from cane. 3. Sweep cane to detect vehicle vibrations and patterns. 4. Confirm crosswalk presence and safety through paving. 5. Cross with steady pace while maintaining cane sweeps. </ego\_plan>

<exo\_verify> Plan is consistent: Cane positioning detects curb (frame 47), tactile paving visible (frame 52), and traffic patterns allow safe crossing. Visual confirmation shows clear crosswalk and minimal traffic in current direction. </exo\_verify>

<answer> Cross when traffic is clear, using cane to detect curb edge and tactile paving for guidance. Maintain steady pace with continuous cane sweep. </answer>

<ego\_plan> 1. Progress systematically along vine rows to next pruning section. 2. Identify dead/dry branches requiring removal on vines. 3. Cut branches at structural joints near main stems using pruning shears. 4. Check that branches are properly removed and no debris remains on vines 5. Complete current section and prepare to move to next row. </ego\_plan>

<exo\_verify> Plan is consistent: Video shows sequential row navigation (frame 3), targeted branch removal (frame 14), joint-level cutting (frame 43), and methodical progression (frame 156). Matches standard vineyard pruning methodology for winter dormancy management. </exo\_verify></exo\_verify>

<answer> Systematic row-by-row removal of dead branches at structural joints, clearing debris as they progress through the vineyard. </answer>

Figure 6. **EgoVITA Qualitative Examples. Left:** For a blind person, the <ego\_plan> generates sequential, safety-critical actions. **Right:** For a procedural task, the <ego\_plan> specifies a systematic, step-by-step approach. In both cases, the <exo\_verify> block confirms the plan's consistency with key visual frames, leading to a grounded and actionable <answer>.

Table 5. **Anticipatory** (**ACMG**) **vs. Present Grounding.** We compare ACMG with a *present-frame* baseline (grounding on frame t). While both improve over the baseline, ACMG delivers substantially stronger gains, highlighting its role in procedural reasoning.

Model	EgoBlind	EgoPlan	EgoThink	EOC-Bench
Qwen2.5-VL-7B	29.7	30.2	48.2	41.6
Present	33.8 (+4.1)	31.2 (+1.0)	50.1 (+1.9)	42.8 (+1.2)
ACMG	37.4 (+7.7)	32.9 (+2.7)	51.9 (+3.7)	44.1 (+2.5)

Table 6. **Ablation on Trainable Vision Components.** We analyze training the vision encoder (VE) and vision projector (MLP) with DoRA adapters. The LLM is always trained during GRPO.

Components Trained			Egocentric Benchmarks				
Model	VE	MLP	LLM	EgoBlind	EgoPlan	EgoThink	EOC-Bench
Qwen2.5-VL-7B	Х	Х	Х	29.7	30.2	48.2	41.6
Frozen Vision Pipeline	Х	Х	1	32.1 (+2.4)	30.8 (+0.6)	48.9 (+0.7)	42.0 (+0.4)
Adaptive Projector	X	1	1	34.2 (+4.5)	31.5 (+1.3)	50.1 (+1.9)	42.8 (+1.2)
Adaptive Encoder	1	X	1	35.8 (+6.1)	32.1 (+1.9)	50.8 (+2.6)	43.2 (+1.6)
EgoVITA (Full)	1	1	1	37.4 (+7.7)	32.9 (+2.7)	51.9 (+3.7)	44.1 (+2.5)

to anticipate what will happen next, rather than just describe what is currently visible. This helps the model link each planned action to its future visual outcome, fostering a predictive understanding of how tasks unfold over time. For comparison, present-frame grounding measures similarity between the predicted visual feature and the current frame,  $sim(\hat{v}_i, v_t)$ , which only encourages the model to describe what is currently visible. In contrast, ACMG connects each plan clause  $c_i$  to future visual states  $v_{t+n}$  by computing  $\max_{n=1}^{N} \sin(\hat{v}_i, v_{t+n})$ , encouraging the model to predict the visual consequences of its actions and select the bestaligned frame. As shown in Table 5, models trained with only present-frame grounding show limited improvement because they focus on describing the current scene rather than learning the causal effects of actions. ACMG explicitly enforces this prediction; however, visual grounding alone is insufficient: a plan might be predictive but still illogical (e.g., "Grasp the hot pan"). The <exo\_verify> stage, guided by

the confidence reward, corrects such errors by enforcing logical consistency. Together, ACMG and confidence produce plans that are both visually grounded and logically coherent.

**RQ5:** How does training different vision components affect egocentric reasoning? Table 6 shows that joint adaptation of all vision components is critical for strong performance. Training with a *frozen vision pipeline* yields the smallest gain (+2.4 on EgoBlind) as the visual features are static. Adapting only the *projector* improves alignment (+4.5), while adapting only the *encoder* yields a larger gain (+6.1) but can lead to conflicts between the encoder outputs and the downstream projector. The best performance (+7.7) is achieved by jointly training both encoder and projector (*Full*), demonstrating that complete end-to-end visual adaptation is necessary for robust egocentric reasoning.

# 5. Conclusion

We presented EgoVITA, a framework that improves egocentric video reasoning by enhancing procedural reasoning. We achieve this by disentangling the task into egocentric planning and exocentric verification. This two-stage approach enables view-invariant learning, yielding strong gains on egocentric benchmarks while maintaining and improving performance on exocentric video tasks. Future work will extend this framework to support streaming, continuous egocentric scenarios.

# Acknowledgments

This research was supported by the National Eye Institute (NEI) of the National Institutes of Health (NIH) under award number R01EY034562. The content is solely the responsibility of the authors and does not necessarily represent the official views of the NIH.

# References

- [1] Shuai Bai, Keqin Chen, Xuejing Liu, Jialin Wang, Wenbin Ge, Sibo Song, Kai Dang, Peng Wang, Shijie Wang, Jun Tang, et al. Qwen2. 5-vl technical report. *arXiv preprint arXiv:2502.13923*, 2025. 3, 5, 15, 16
- [2] Siddhant Bansal, Chetan Arora, and CV Jawahar. My view is the best view: Procedure learning from egocentric videos. In European Conference on Computer Vision (ECCV), pages 657–675, 2022. 3, 5, 15
- [3] Marius Bock, Hilde Kuehne, Kristof Van Laerhoven, and Michael Moeller. Wear: An outdoor sports dataset for wearable and egocentric activity recognition. In *Proceedings of* the ACM on Interactive, Mobile, Wearable and Ubiquitous Technologies (IMWUT), pages 1–21, 2024. 1
- [4] Yi Chen, Yuying Ge, Yixiao Ge, Mingyu Ding, Bohao Li, Rui Wang, Ruifeng Xu, Ying Shan, and Xihui Liu. Egoplanbench: Benchmarking multimodal large language models for human-level planning. *arXiv preprint arXiv:2312.06722*, 2023. 5, 7, 13
- [5] Sijie Cheng, Zhicheng Guo, Jingwen Wu, Kechen Fang, Peng Li, Huaping Liu, and Yang Liu. Egothink: Evaluating firstperson perspective thinking capability of vision-language models. In *Proceedings of the IEEE/CVF Conference on Computer Vision and Pattern Recognition (CVPR)*, pages 14291–14302, 2024. 5
- [6] Chaoyou Fu, Yuhan Dai, Yongdong Luo, Lei Li, Shuhuai Ren, Renrui Zhang, Zihan Wang, Chenyu Zhou, Yunhang Shen, Mengdan Zhang, et al. Video-mme: The first-ever comprehensive evaluation benchmark of multi-modal llms in video analysis. In *Proceedings of the Computer Vision and Pattern Recognition Conference (CVPR)*, pages 24108–24118, 2025. 5
- [7] Mohsen Gholami, Ahmad Rezaei, Zhou Weimin, Yong Zhang, and Mohammad Akbari. Spatial reasoning with vision-language models in ego-centric multi-view scenes. *arXiv* preprint arXiv:2509.06266, 2025. 1, 2

- [8] Daya Guo, Dejian Yang, Haowei Zhang, Junxiao Song, Ruoyu Zhang, Runxin Xu, Qihao Zhu, Shirong Ma, Peiyi Wang, Xiao Bi, et al. Deepseek-r1: Incentivizing reasoning capability in llms via reinforcement learning. arXiv preprint arXiv:2501.12948, 2025. 2
- [9] Yuping He, Yifei Huang, Guo Chen, Baoqi Pei, Jilan Xu, Tong Lu, and Jiangmiao Pang. Egoexobench: A benchmark for firstand third-person view video understanding in mllms. In Advances in Neural Information Processing Systems (NeurIPS), 2025. 1, 2
- [10] Sihong Huang, Jiaxin Wu, Xiaoyong Wei, Yi Cai, Don San Jiang, and Yaowei Wang. Sound bridge: Associating egocentric and exocentric videos via audio cues. In *Proceedings of the Computer Vision and Pattern Recognition Conference* (CVPR), pages 28942–28951, 2025. 2
- [11] Aaron Hurst, Adam Lerer, Adam P Goucher, Adam Perelman, Aditya Ramesh, Aidan Clark, AJ Ostrow, Akila Welihinda, Alan Hayes, Alec Radford, et al. Gpt-4o system card. *arXiv* preprint arXiv:2410.21276, 2024. 7, 14
- [12] Ji Hyeok Jung, Eun Tae Kim, Seoyeon Kim, Joo Ho Lee, Bumsoo Kim, and Buru Chang. Is 'right'right? enhancing object orientation understanding in multimodal large language models through egocentric instruction tuning. In *Proceedings* of the Computer Vision and Pattern Recognition Conference (CVPR), pages 14257–14267, 2025. 1, 2
- [13] Minjoon Jung, Junbin Xiao, Junghyun Kim, Byoung-Tak Zhang, and Angela Yao. Egoexo-con: Exploring viewinvariant video temporal understanding. arXiv preprint arXiv:2510.26113, 2025. 2
- [14] Junhyeok Kim, Jaewoo Park, Junhee Park, Sangeyl Lee, Ji-wan Chung, Jisung Kim, Ji Hoon Joung, and Youngjae Yu. Guidedog: A real-world egocentric multimodal dataset for blind and low-vision accessibility-aware guidance. arXiv preprint arXiv:2503.12844, 2025. 1, 2
- [15] Yogesh Kulkarni and Pooyan Fazli. Videosavi: Self-aligned video language models without human supervision. In Conference on Language Modeling (COLM), 2024. 2
- [16] Yogesh Kulkarni and Pooyan Fazli. Avatar: Reinforcement learning to see, hear, and reason over video. arXiv preprint arXiv:2508.03100, 2025. 2
- [17] Yogesh Kulkarni and Pooyan Fazli. Videopasta: 7k preference pairs that matter for video-llm alignment. In *Conference on Empirical Methods in Natural Language Processing* (EMNLP), 2025. 2
- [18] Kunchang Li, Yali Wang, Yinan He, Yizhuo Li, Yi Wang, Yi Liu, Zun Wang, Jilan Xu, Guo Chen, Ping Luo, et al. Mvbench: A comprehensive multi-modal video understanding benchmark. In Proceedings of the IEEE/CVF Conference on Computer Vision and Pattern Recognition (CVPR), pages 22195–22206, 2024. 5
- [19] Yuxuan Li, Vijay Veerabadran, Michael L Iuzzolino, Brett D Roads, Asli Celikyilmaz, and Karl Ridgeway. Egotom: Benchmarking theory of mind reasoning from egocentric videos. *arXiv preprint arXiv:2503.22152*, 2025. 1, 2
- [20] Shuo Liang, Yiwu Zhong, Zi-Yuan Hu, Yeyao Tao, and Liwei Wang. Fine-grained spatiotemporal grounding on egocentric videos. In *Proceedings of the IEEE/CVF international* conference on computer vision (ICCV), 2025. 1, 2

- [21] Shuo Liang, Yiwu Zhong, Zi-Yuan Hu, Yeyao Tao, and Liwei Wang. Fine-grained spatiotemporal grounding on egocentric videos. In *Proceedings of the IEEE/CVF international conference on computer vision (ICCV)*, 2025. 1
- [22] Shih-Yang Liu, Chien-Yi Wang, Hongxu Yin, Pavlo Molchanov, Yu-Chiang Frank Wang, Kwang-Ting Cheng, and Min-Hung Chen. Dora: Weight-decomposed low-rank adaptation. In Forty-first International Conference on Machine Learning (ICML), 2024. 5
- [23] Mi Luo, Zihui Xue, Alex Dimakis, and Kristen Grauman. Viewpoint rosetta stone: Unlocking unpaired ego-exo videos for view-invariant representation learning. In *Proceedings* of the Computer Vision and Pattern Recognition Conference (CVPR), pages 15802–15812, 2025. 2
- [24] Lorenzo Mur-Labadia, Maria Santos-Villafranca, Jesus Bermudez-Cameo, Alejandro Perez-Yus, Ruben Martinez-Cantin, and Jose J. Guerrero. O-mama: Learning object mask matching between egocentric and exocentric views. In Proceedings of the IEEE/CVF international conference on computer vision (ICCV), 2025. 2
- [25] Baoqi Pei, Yifei Huang, Jilan Xu, Yuping He, Guo Chen, Fei Wu, Yu Qiao, and Jiangmiao Pang. Egothinker: Unveiling egocentric reasoning with spatio-temporal cot. In Advances in Neural Information Processing Systems (NeurIPS), 2025. 2, 6
- [26] Taiying Peng, Jiacheng Hua, Miao Liu, and Feng Lu. In the eye of mllm: Benchmarking egocentric video intent understanding with gaze-guided prompting. In Advances in Neural Information Processing Systems (NeurIPS), 2025. 1, 2
- [27] Toby Perrett, Ahmad Darkhalil, Saptarshi Sinha, Omar Emara, Sam Pollard, Kranti Kumar Parida, Kaiting Liu, Prajwal Gatti, Siddhant Bansal, Kevin Flanagan, et al. Hd-epic: A highlydetailed egocentric video dataset. In *Proceedings of the Computer Vision and Pattern Recognition Conference (CVPR)*, pages 23901–23913, 2025. 1, 2, 3, 5, 15, 18
- [28] Chiara Plizzari, Alessio Tonioni, Yongqin Xian, Achin Kulshrestha, and Federico Tombari. Omnia de egotempo: Benchmarking temporal understanding of multi-modal llms in egocentric videos. In *Proceedings of the Computer Vision and Pattern Recognition Conference (CVPR)*, pages 24129–24138, 2025. 1, 2
- [29] Rafael Rafailov, Archit Sharma, Eric Mitchell, Christopher D Manning, Stefano Ermon, and Chelsea Finn. Direct preference optimization: Your language model is secretly a reward model. In Advances in Neural Information Processing Systems (NeurIPS), pages 53728–53741, 2023. 2
- [30] Ashish Seth, Utkarsh Tyagi, Ramaneswaran Selvakumar, Nishit Anand, Sonal Kumar, Sreyan Ghosh, Ramani Duraiswami, Chirag Agarwal, and Dinesh Manocha. Egoillusion: Benchmarking hallucinations in egocentric video understanding. In Conference on Empirical Methods in Natural Language Processing (EMNLP), 2025. 1, 2
- [31] Ziyao Shangguan, Chuhan Li, Yuxuan Ding, Yanan Zheng, Yilun Zhao, Tesca Fitzgerald, and Arman Cohan. Tomato: Assessing visual temporal reasoning capabilities in multimodal foundation models. In *Proceedings of the International Con*ference on Learning Representations (ICLR), 2025. 5

- [32] Pengzhan Sun, Junbin Xiao, Tze Ho Elden Tse, Yicong Li, Arjun Akula, and Angela Yao. Visual intention grounding for egocentric assistants. In arXiv preprint arXiv:2504.13621, 2025. 1, 2
- [33] Shulin Tian, Ruiqi Wang, Hongming Guo, Penghao Wu, Yuhao Dong, Xiuying Wang, Jingkang Yang, Hao Zhang, Hongyuan Zhu, and Ziwei Liu. Ego-r1: Chain-of-tool-thought for ultra-long egocentric video reasoning. *arXiv* preprint arXiv:2506.13654, 2025. 2
- [34] Ashwin Vinod, Shrey Pandit, Aditya Vavre, and Linshen Liu. Egovlm: Policy optimization for egocentric video understanding. arXiv preprint arXiv:2506.03097, 2025. 2, 6
- [35] Weiyun Wang, Zhangwei Gao, Lixin Gu, Hengjun Pu, Long Cui, Xingguang Wei, Zhaoyang Liu, Linglin Jing, Shenglong Ye, Jie Shao, et al. Internvl3. 5: Advancing open-source multimodal models in versatility, reasoning, and efficiency. arXiv preprint arXiv:2508.18265, 2025. 5
- [36] Weihan Wang, Zehai He, Wenyi Hong, Yean Cheng, Xiaohan Zhang, Ji Qi, Ming Ding, Xiaotao Gu, Shiyu Huang, Bin Xu, et al. Lvbench: An extreme long video understanding benchmark. In *Proceedings of the IEEE/CVF International Conference on Computer Vision (ICCV)*, pages 22958–22967, 2025. 5
- [37] Junbin Xiao, Nanxin Huang, Hao Qiu, Zhulin Tao, Xun Yang, Richang Hong, Meng Wang, and Angela Yao. Egoblind: Towards egocentric visual assistance for the blind people. In Advances in Neural Information Processing Systems (NeurIPS), 2025. 1, 2, 5
- [38] Jun Xu, Tao Mei, Ting Yao, and Yong Rui. Msr-vtt: A large video description dataset for bridging video and language. In *Proceedings of the IEEE conference on computer vision and pattern recognition (CVPR)*, pages 5288–5296, 2016. 5
- [39] Jilan Xu, Yifei Huang, Baoqi Pei, Junlin Hou, Qingqiu Li, Guo Chen, Yuejie Zhang, Rui Feng, and Weidi Xie. Egoexogen: Ego-centric video prediction by watching exo-centric videos. In *International Conference on Learning Representa*tions (ICLR), 2025. 2
- [40] Jingkang Yang, Shuai Liu, Hongming Guo, Yuhao Dong, Xiamengwei Zhang, Sicheng Zhang, Pengyun Wang, Zitang Zhou, Binzhu Xie, Ziyue Wang, et al. Egolife: Towards egocentric life assistant. In Proceedings of the Computer Vision and Pattern Recognition Conference (CVPR), pages 28885–28900, 2025. 1, 2, 5
- [41] Hanrong Ye, Haotian Zhang, Erik Daxberger, Lin Chen, Zongyu Lin, Yanghao Li, Bowen Zhang, Haoxuan You, Dan Xu, Zhe Gan, et al. Mm-ego: Towards building egocentric multimodal llms for video qa. In *International Conference* on Learning Representations (ICLR), 2025. 2
- [42] Yuqian Yuan, Ronghao Dang, Long Li, Wentong Li, Dian Jiao, Xin Li, Deli Zhao, Fan Wang, Wenqiao Zhang, Jun Xiao, et al. Eoc-bench: Can mllms identify, recall, and forecast objects in an egocentric world? In Advances in Neural Information Processing Systems (NeurIPS), 2025. 1, 2, 5
- [43] Haoyu Zhang, Qiaohui Chu, Meng Liu, Yunxiao Wang, Bin Wen, Fan Yang, Tingting Gao, Di Zhang, Yaowei Wang, and Liqiang Nie. Exo2ego: Exocentric knowledge guided mllm for egocentric video understanding. *arXiv preprint arXiv:2503.09143*, 2025. 2

- [44] Amy Zhao, Chengcheng Tang, Lezi Wang, Yijing Li, Mihika Dave, Lingling Tao, Christopher D. Twigg, and Robert Y. Wang. Egobody3m: Egocentric body tracking on a vr headset using a diverse dataset. In *European Conference on Computer Vision (ECCV)*, page 375–392, 2024. 1
- [45] Yuze Zhao, Jintao Huang, Jinghan Hu, Xingjun Wang, Yunlin Mao, Daoze Zhang, Zeyinzi Jiang, Zhikai Wu, Baole Ai, Ang Wang, et al. Swift: a scalable lightweight infrastructure for fine-tuning. In *Proceedings of the AAAI Conference on Artificial Intelligence (AAAI)*, pages 29733–29735, 2025. 5
- [46] Sheng Zhou, Junbin Xiao, Qingyun Li, Yicong Li, Xun Yang, Dan Guo, Meng Wang, Tat-Seng Chua, and Angela Yao. Egotextvqa: Towards egocentric scene-text aware video question answering. In *Proceedings of the Computer Vision and Pattern Recognition Conference (CVPR)*, pages 3363–3373, 2025. 1, 2
- [47] Yichen Zhu and Feifei Feng. Let me show you: Learning by retrieving from egocentric video for robotic manipulation. In *IEEE/RSJ International Conference on Intelligent Robots and Systems (IROS)*, 2025. 1

# **Appendix**

# A. Ablation Studies

**RQ1:** Why Max Instead of Average Pooling for  $R_{\rm ACMG}$ ? A valid concern is that max pooling (Eq. 6) could reward spurious, high-similarity outliers, whereas a mean pooling operation might better capture durational events (e.g., "walk to the bus stop"). In Table 7, we directly ablate this by replacing max pooling with mean pooling across the N=16 future frames. The results show that mean pooling is significantly less effective, providing only a fraction of the performance gain (e.g., +3.8 vs. +7.7 on EgoBlind, and +1.9 vs. +3.7 on EgoThink).

The *mean* operation's weakness is that it **dilutes the reward signal**. A correct durational clause like "walk to the bus stop" will have high similarity with *some*, but not necessarily all, of the N=16 future frames. Averaging across the entire window (including the non-matching frames) punishes this correct, but sparse, temporal alignment, resulting in a weak, non-descriptive reward. In contrast, max pooling is "robust to temporal shifts" because it finds the **peak evidence** that the predicted event did occur within the window, regardless of its exact timing or duration. This provides a much stronger and more stable learning signal for grounding, and the empirical results suggest this benefit outweighs the risk of spurious outliers.

**RQ2:** Is the teacher-guided warm-up phase necessary for the confidence reward? Table 8 examines the effect of removing the 200-step teacher-guided warm-up phase from the confidence reward. Without this initialization, the model relies solely on self-ranking from the start of training. Results show that removing the warm-up phase leads to modest performance drops across all benchmarks: -1.4 on EgoBlind, -1.1 on EgoPlan, -1.4 on EgoThink, and -1.1 on EOC-Bench. While the model still achieves substantial gains over the baseline without teacher guidance, the warm-up phase provides a useful initialization that helps the model learn stable verification patterns before transitioning to self-improvement.

The teacher-guided phase grounds the model in highquality reasoning examples, preventing early-stage instability where the model might reinforce suboptimal verification strategies. However, the relatively small performance gap suggests that the self-ranking mechanism is robust enough to learn effective verification even without explicit teacher supervision, indicating that the strong gains stem from the confidence reward structure itself rather than solely from teacher distillation.

**RQ3:** Impact of Exocentric Regularization. Figure 7 demonstrates the importance of exocentric regularization for preventing catastrophic forgetting. Training on egocentric data via SFT causes an initial performance drop on exocentric benchmarks, as seen by the 'RL Step 0' (SFT) perfor-

Table 7. **Ablation on ACMG Pooling Strategy.** We compare Max Pooling (used in EgoVITA) against Mean Pooling for the  $R_{ACMG}$  reward. Results on Qwen2.5-VL-7B.

	Egocentric Benchmarks					
ACMG Variant	EgoBlind	EgoPlan	EgoThink	EOC-Bench		
Qwen2.5-VL-7B	29.7	30.2	48.2	41.6		
R <sub>ACMG</sub> (Mean Pooling)	33.5 (+3.8)	31.5 (+1.3)	50.1 (+1.9)	42.6 (+1.0)		
$R_{ACMG}$ (Max Pooling) (EgoVITA)	37.4 (+7.7)	32.9 (+2.7)	51.9 (+3.7)	44.1 (+2.5)		

Table 8. **Ablation on Teacher-Guided Warm-up Duration.** We analyze the effect of removing the 200-step teacher-guided phase from the confidence reward. Results on Qwen2.5-VL-7B.

	Egocentric Benchmarks					
Variant	EgoBlind	EgoPlan	EgoThink	EOC-Bench		
Qwen2.5-VL-7B	29.7	30.2	48.2	41.6		
No Teacher Warm-up (0 steps)  EgoVITA (200 steps)		31.8 (+1.6) 32.9 (+2.7)		43.0 (+1.4) 44.1 (+2.5)		

mance being below the 'Base Model' across all four tasks. This drop occurs because SFT overfits to the egocentric data distribution. Without intervention, this forgetting continues, as shown by the 'w/o Regularization', where performance progressively degrades. In contrast, EgoVITA's regularization, which interleaves GRPO updates with training on a held-out exocentric dataset, reverses this trend. The model not only recovers from the initial SFT drop but ultimately improving upon the original base model's performance. This confirms that our approach enables the model to specialize in egocentric reasoning while preserving and even enhancing its general exocentric understanding, tackling a key challenge in ego-exo knowledge transfer.

**RQ4: Sensitivity to Anticipation Window** N. We analyze the sensitivity of  $R_{ACMG}$  to N, the number of future frames used for grounding, in Table 9. Performance is clearly sensitive to this hyperparameter. A small window, such as N=4or N=8, yields lower gains. This is because the anticipation window is too myopic: a correct plan clause (e.g., "Grab the bottle") may not have its corresponding visual outcome (the bottle being grabbed) appear within such a short temporal window, unfairly penalizing valid long-term plans. Conversely, a large window (N = 32) also degrades performance compared to our chosen value.  $R_{ACMG}$  relies on a  $\max$  operation over the N future frames to find the best-aligned visual state. A window that is too large makes this signal noisy, increasing the risk of rewarding a spurious or coincidental visual match that is not causally linked to the  $ego_plan> clause$ . Therefore, N=16 represents an effective balance, providing a flexible enough window to handle temporal shifts in actions while remaining focused enough to reward precise, causal predictions.

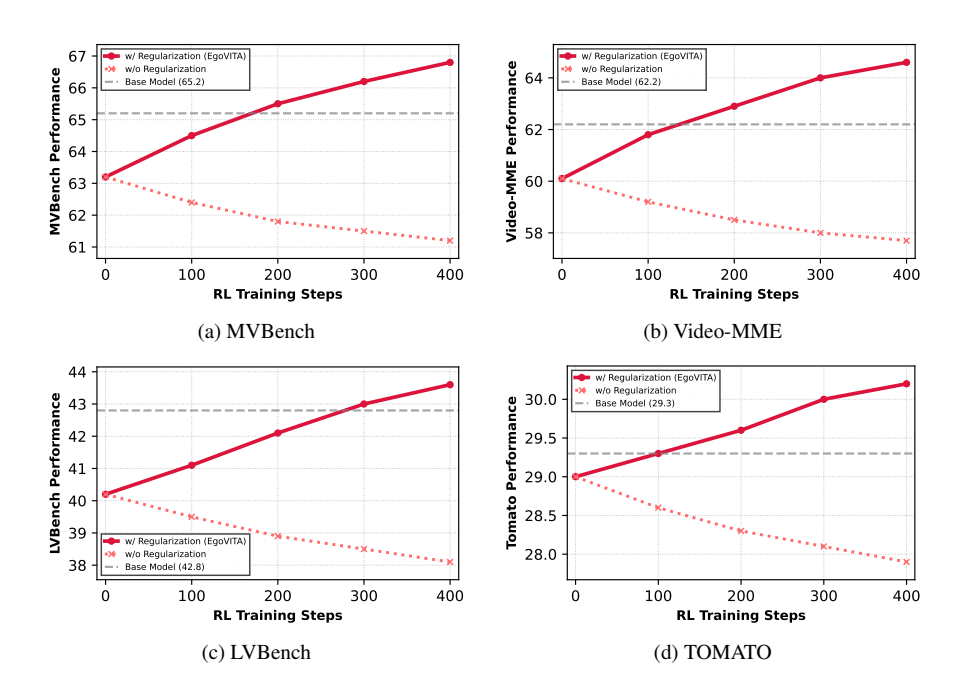


Figure 7. **Ablation on Exocentric Regularization.** The plots show performance on four exocentric benchmarks (Qwen2.5-VL family). Training on egocentric data via SFT causes an initial performance drop, or catastrophic forgetting. Without regularization, this decline continues. EgoVITA's exocentric regularization reverses this forgetting, recovering performance and ultimately improving upon the original base model.

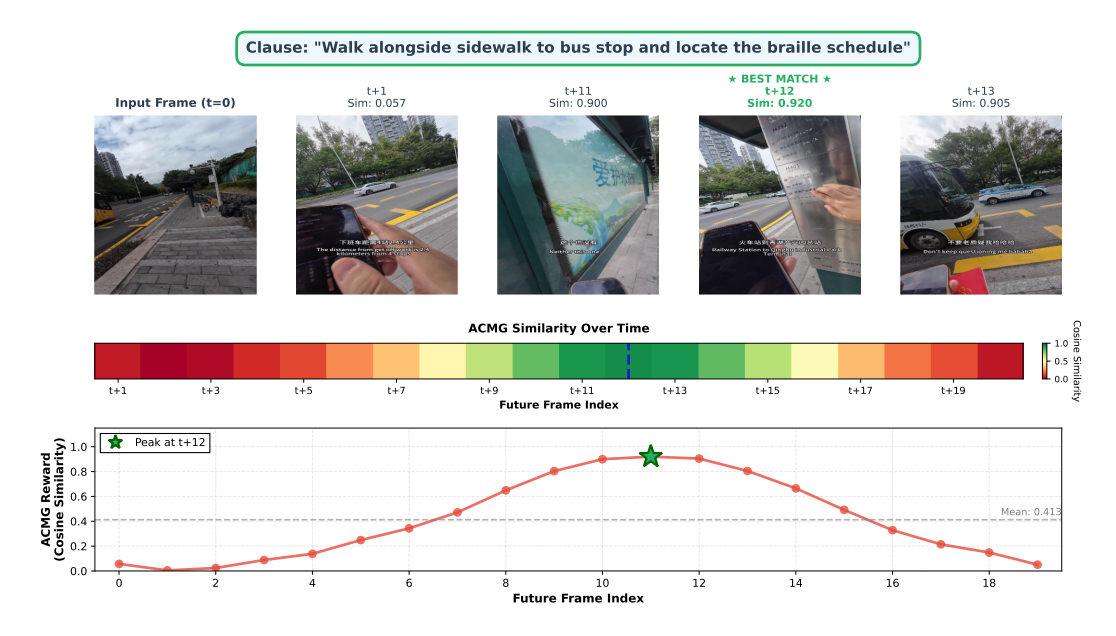


Figure 8.  $R_{\rm ACMG}$  Temporal Grounding for a Single Clause. Given the clause "Walk alongside sidewalk to bus stop and locate the braille schedule," the Anticipation Head projects it into visual space and computes cosine similarity with future frames. The best match occurs at t+12 (Sim: 0.920) when the braille sign appears. The heatmap and curve show similarity peaks at the temporally correct frame, demonstrating that  $R_{\rm ACMG}$  rewards clauses that accurately predict future visual states.

**RQ5:** How does  $R_{ACMG}$  reward vary across clause positions? We analyze  $500 < ego\_plan > samples$  from Ego-Plan [4], which naturally decompose into five semantic posi-

tions: (1) Move (approach), (2) Locate (target identification), (3) Action (perform task), (4) Verify (state confirmation), and (5) Complete (goal achievement). Clauses are tagged into the

Table 9. Ablation on Anticipation Window (N). We analyze the sensitivity of the ACMG reward to N, the number of future frames used for grounding. Results on Qwen2.5-VL-7B. N=16 provides the best balance, as smaller windows are too myopic to capture delayed actions, while larger windows introduce noisy, spurious correlations.

		Egocentric	Benchmark	xs .
N (Future Frames)	EgoBlind	EgoPlan	EgoThink	EOC-Bench
Qwen2.5-VL-7B	29.7	30.2	48.2	41.6
N=4 (Too Myopic)	32.0 (+2.3)	31.0 (+0.8)	49.3 (+1.1)	42.4 (+0.8)
N = 8	35.1 (+5.4)	32.1 (+1.9)	50.8 (+2.6)	43.4 (+1.8)
N = 16 (EgoVITA)	37.4 (+7.7)	32.9 (+2.7)	51.9 (+3.7)	44.1 (+2.5)
N=32 (Too Noisy)	36.2 (+6.5)	32.5 (+2.3)	51.3 (+3.1)	43.7 (+2.1)

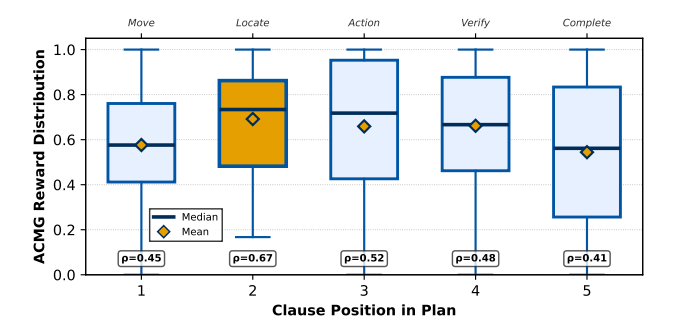


Figure 9. ACMG Reward Distribution by Clause Position. Box plots show ACMG reward distributions for the first five clauses in <ego\_plan> sequences. Top labels indicate typical semantic roles at each position. Middle clauses (positions 2-3) achieve higher rewards and stronger correlation  $(\rho)$  with answer correctness, demonstrating that ACMG effectively distinguishes between concrete action steps and abstract reasoning phases.

five action categories using GPT-4o [11]. These categories are not rigid but reflects a common semantic structure in procedural tasks. Figure 8 provides a detailed visualization of  $R_{\rm ACMG}$  grounding for a single clause, while Figure 9 shows that  $R_{\rm ACMG}$  provides position-sensitive grounding signals. Middle clauses (positions 2–3: corresponding to target localization and action execution) receive significantly higher  $R_{\rm ACMG}$  rewards (mean = 0.67–0.69) and show stronger correlations with final answer correctness ( $\rho=0.52$ –0.67) compared to navigation (position 1,  $\rho=0.45$ ) or completion steps (position 5,  $\rho=0.41$ ).

This variation demonstrates that  $R_{\rm ACMG}$  is adaptively selective, providing stronger grounding signals for visually concrete actions while appropriately moderating rewards for abstract planning phases. The correlation pattern validates that  $R_{\rm ACMG}$  focuses on task-critical visual grounding, i.e., clauses with higher  $R_{\rm ACMG}$  rewards are indeed more predictive of correct final answers, confirming that the reward mechanism aligns with meaningful task structure rather than

Table 10. Anticipation Head Architecture. The MLP projects text embeddings  $(D_{llm})$  to the visual space  $(D_{vis})$ .

Stage	Operation	Output Shape
Input	_	$B \times D_{llm}$
Layer 1	Linear Projection	$B \times D_{hidden}$
Activation	GELU	$B \times D_{hidden}$
Normalization	LayerNorm	$B \times D_{hidden}$
Layer 2	Linear Projection	$B \times D_{vis}$

providing noisy uniform feedback.

# **B.** Anticipation Head Architecture

The Anticipation Head Table 10 is a lightweight, two-layer Multilayer Perceptron (MLP) designed to project the LLM's hidden textual states into the shared visual embedding space. It consists of a down-projection linear layer, a GELU activation function, and a final linear layer that maps to the visual encoder's output dimension. We apply Layer Normalization pre-activation to stabilize training. This simple design enables efficient cross-modal alignment without introducing significant computational overhead.

# C. Qualitative Examples

We provide a direct comparison between EgoVITA and the Qwen2.5-VL-7B in Figure 10, illustrating how our two-stage architecture resolves common MLLM failure modes in egocentric reasoning.

In the Kitchen Cleanup example (Left), the baseline fails to ground its reasoning in the visual evidence. It exhibits temporal hallucination by adding a "cabinet storage" step that never occurs and spatial misalignment by ignoring the actual sink washing process shown in the video. Consequently, it provides a plausible but incorrect recommendation to "skip checking cleanliness," assuming the dishwasher does everything. EgoVITA, however, generates a grounded plan that prioritizes preconditions. The verification module explicitly cites the "active dish washing" in Frames 6-8 and the "dishwasher space check" in Frame 5, correcting the logic to ensure a systematic and visually consistent cleanup procedure.

In the Baking Process example (Right), the baseline suffers from hallucinations, introducing factual errors (mentioning "eggs" not present in the scene) and spatial misalignment (claiming a "whisk" is used when the video clearly shows a spoon). It further fails in temporal reasoning by suggesting "immediate baking" without the necessary intermediate steps. EgoVITA avoids these pitfalls through its ACMG reward. By predicting the visual features of the next steps (e.g., "Find the appropriate measuring spoon"), the model correctly identifies the fine-grained spoon-flour interaction. The exocentric verification further confirms the "measuring"

action at Frame 18, ensuring the response is strictly faithful to the observed video content.

# **D. Prompt Templates**

To establish robust supervision for our two-stage RL framework, we generate high-quality training data using Qwen2.5-VL-72B [1]. For the egocentric planning stage, we utilize the prompt in Figure 11 to transform raw EgoProceL [2] temporal annotations into structured, step-by-step egocentric plans. Complementing this, the prompt in Figure 12 is applied to the HD-EPIC [27] dataset to generate third-person "exocentric verifications," which teach the model to verify its plans against observable visual evidence.



**Query:** What approach to follow for post-meal kitchen cleanup?

**Qwen2.5-VL-7B:** Put all dishes directly into the dishwasher. The sink isn't needed for this process. The video shows the person putting dishes away in cabinets first. There's no need to check cleanliness since the dishwasher cleans everything.

<ego\_plan> 1. Approach the sink area with used dishes 2. Check dishwasher space and cleaning tools 3. Wash and rinse all food residue from dishes 4. Confirm dishes are thoroughly clean before loading 5. Complete: Load all utensils and close dishwasher.

<exo\_verify> Plan is consistent: Video shows movement to sink (frame 2), dishwasher space check (frame 5), active dish washing (frames 6-8), verification of clean dishes (frame 17), and completion with dishwasher loading (frames 19-21). Matches standard kitchen cleanup methodology for post-meal dish management. </exo\_verify>

<answer> Systematic post-meal cleanup with thorough washing of used dishes, verification of cleanliness, and proper dishwasher loading. </answer>



**Query:** What are the next steps the person followed in the baking process?

**Qwen2.5-VL-7B:** Add eggs to the flour first, then pour the leavening agent. The can contains baking powder that should be added last. The video shows the person using a whisk instead of a spoon. Immediately bake the mixture.

<ego\_plan> 1. Position myself at the kitchen counter with the opened can 2. Find the appropriate measuring spoon from the drawer 3. Measure and add the required amount of powder to the flour 4. Confirm the correct quantity has been added to the mixture 5. Set aside the can and prepare for adding the next ingredient. </ego\_plan>

<exo\_verify> Plan is consistent: Video shows counter positioning with opened can (frame 2), drawer access to locate spoon (frame 11), measuring and adding agent to flour (frames 15-19), verification of proper measurement (frame 18), and preparation for next step (frame 20). </exo\_verify>

<answer> Position at counter, locate measuring spoon, measure and add leavening agent, verify correct amount, and prepare for next ingredient addition. </answer>

Figure 10. **EgoVITA Qualitative Examples.**The baseline Qwen2.5-VL-7B [1] suffers from factual errors and temporal hallucinations (e.g., inventing "cabinet storage" steps or objects like "eggs" and "whisks"). In contrast, EgoVITA utilizes **Egocentric Planning** to correctly sequence fine-grained actions and **Exocentric Verification** to ground them in specific video frames (e.g., "frame 5", "frame 18"), preventing hallucinations and ensuring visual consistency.

# Prompt for Egocentric Planning SFT Data Generation (EgoProceL)

You are an expert in egocentric video understanding and procedural planning. You will be provided with a list of timestamped atomic actions annotated from a first-person video. Your task is to convert these raw annotations into a high-quality instruction-following training sample containing a query, options, and a grounded plan.

Input Data: A list of timestamped actions (Start Time, End Time, Action Description).

#### Your Task:

- 1. **Synthesize a User Query:** Infer the overall goal of the video (e.g., "How do I make brownies?") and formulate it as a question a user would ask for assistance.
- 2. **Generate Answer Options:** Create 4 distinct multiple-choice options (A, B, C, D) that summarize the procedure:
- 3. **One Correct Option:** An accurate summary of the sequential steps.
- 4. **Three Distractors:** Plausible but incorrect summaries (e.g., incorrect order, missing critical steps, or describing a different but related task).
- 5. **Construct the Response:** Generate the target output using the following strictly enforced format:
- 6. <ego-plan>: A numbered, step-by-step plan. Each step must cite the specific timestamp interval from the input to ensure temporal grounding.
- 7. : The final answer containing the correct option letter and its full text.

**Input Annotations:** {50.48-54.7: break egg}, {64.19-76.3: mix eggs}, {87.13-91.1: add water}, ... **Target Output Format:** 

```
[User Query]: {Generated Query}
[Options]:
(A) {Option Text}
(B) {Option Text} ...
[Response]:
<ego_plan>
1. Break the egg into the bowl to start the batter (50.48 - 54.7).
2. Mix the eggs thoroughly using a whisk (64.19 - 76.3).
3. Add water to the mixture as specified (87.13 - 91.1).
...
</ego_plan>
<answer> (A) {Correct Option Text} </answer>
```

Figure 11. Prompt used to transform raw temporal annotations into structured SFT samples for egocentric planning. This prompts the teacher model (Qwen2.5-VL-72B) to generate a grounded <ego\_plan> and a correct <answer>.

# Prompt for Exocentric Verification SFT Data Generation (HD-EPIC)

You are an intelligent video reasoning assistant. You are provided with an egocentric video and a set of fine-grained, timestamped action annotations. Your goal is to synthesize a reasoning chain that not only plans the actions but also **verifies** them against visual evidence.

### **Input Data:**

- 1. Video Context: An egocentric video clip.
- 2. **Annotations:** A list of atomic actions with start/end timestamps (e.g., "13.73-14.11: flip the bottom part of the coffee machine"). **Your Task:** Generate a structured output containing two distinct blocks:
- 1. <ego\_plan>: Convert the annotations into a coherent, first-person procedural plan. Merge closely related atomic actions into logical steps where appropriate.
- <exo\_verify>: Act as an external auditor. For the plan you just generated, provide a visual verification rationale. Explicitly
  cite visual evidence (objects, hand-object interactions, and state changes) that confirms the plan is actually occurring in the
  video.

**Input Annotations (Example):** {14.2-14.55: Put mug under nozzle}, {14.81-15.08: Pick up coffee capsule}, {16.08-17.26: Slide capsule into gap}...

### **Target Output Format:**

```
[User Query]: How do I prepare the coffee machine for brewing?
[Response]:
<ego_plan>
1. Place the mug under the coffee machine nozzle (14.2 - 14.55).
2. Pick up the coffee capsule from the left countertop (14.81 - 15.08).
3. Insert the capsule into the machine's slot (16.08 - 17.26).
...
</ego_plan>
<exo_verify>
The plan is visually consistent. At 14.5s, the right hand is clearly visible placing the white mug under the spout. The interaction with the capsule is confirmed by the hand trajectory moving from the counter (14.9s) to the machine's top slot (16.5s), followed by the lever being pulled down to lock it.
</exo_verify>
```

Figure 12. The prompt used to generate the exocentric verification data from HD-EPIC [27] annotations. This teaches the model to not only list actions but to ground them in observable visual evidence.